THE FASEB JOURNAL • RESEARCH • www.fasebj.org

Robot-assisted mechanical therapy attenuates stroke-induced limb skeletal muscle injury

Chandan K. Sen,[1] Savita Khanna,[1] Hallie Harris, Richard Stewart, Maria Balch, Mallory Heigel, Seth Teplitsky, Surya Gnyawali, and Cameron Rink[2]

Department of Surgery, Davis Heart and Lung Research Institute, The Ohio State University Wexner Medical Center, Columbus, Ohio, USA

ABSTRACT: The efficacy and optimization of poststroke physical therapy paradigms is challenged in part by a lack of objective tools available to researchers for systematic preclinical testing. This work represents a maiden effort to develop a robot-assisted mechanical therapy (RAMT) device to objectively address the significance of mechanical physiotherapy on poststroke outcomes. Wistar rats were subjected to right hemisphere middle-cerebral artery occlusion and reperfusion. After 24 h, rats were split into control ($RAMT^-$) or $RAMT^+$ groups (30 min daily RAMT over the stroke-affected gastrocnemius) and were followed up to poststroke d 14. $RAMT^+$ increased perfusion 1.5-fold in stroke-affected gastrocnemius as compared to $RAMT^-$ controls. Furthermore, $RAMT^+$ rats demonstrated improved poststroke track width (11% wider), stride length (21% longer), and travel distance (61% greater), as objectively measured using software-automated testing platforms. Stroke injury acutely increased myostatin (3-fold) and lowered brain-derived neurotrophic factor (BDNF) expression (0.6-fold) in the stroke-affected gastrocnemius, as compared to the contralateral one. RAMT attenuated the stroke-induced increase in myostatin and increased BDNF expression in skeletal muscle. Additional RAMT-sensitive myokine targets in skeletal muscle (IL-1ra and IP-10/CXCL10) were identified from a cytokine array. Taken together, outcomes suggest stroke acutely influences signal transduction in hindlimb skeletal muscle. Regimens based on mechanical therapy have the clear potential to protect hindlimb function from such adverse influence.—Sen, C. K., Khanna, S., Harris, H., Stewart, R., Balch, M., Heigel, M., Teplitsky, S., Gnyawali, S., Rink, C. Robot-assisted mechanical therapy attenuates stroke-induced limb skeletal muscle injury. FASEB J. 31, 927–936 (2017). www.fasebj.org

KEY WORDS: ischemia · rehabilitation · physical therapy · cerebrovascular accident

Focal brain ischemia is a leading cause of long-term disability in the United States (1), with more than 25% of stroke survivors afflicted by disability that requires dependence on caregivers for simple activities of daily living (2). Stroke survivors rely on neurophysiological rehabilitation to facilitate restoration of stroke-induced loss of motor function (3). In Western practice, the most commonly applied stroke rehabilitation approach is the Bobath concept (4). However, recent meta-analyses and direct comparisons of the Bobath concept to other rehabilitation paradigms have found no benefit (5). Furthermore, many of the current guidelines for poststroke rehabilitation lack research evidence, leading some to refer to stroke rehabilitative practices as a "black box" (6). Adding to the challenge of evidence-based rehabilitation research in the clinical setting is the heterogeneity of the human stroke disease and complex systems of rehabilitative care that differ in philosophical approach and practice across medical centers (3).

Massage therapy, reliant on mechanotransduction, is a complementary alternative medicine rehabilitation approach. In the United States, it is estimated that more than 18 million adults use massage therapy on an annual basis (7). In the context of care for stroke survivors, massage therapy is more widely practiced in Asia (8). Massage therapy is reported to attenuate inflammation (9), improve local tissue perfusion (10), and reduce tissue stiffness (11). Quantitative outcomes and evidence-based research on underlying mechanisms are scant, however. In this work, we report a novel device aimed at robot-assisted mechanical therapy (RAMT). The objective is to enable the reproducible study of mechanical therapy in a preclinical stroke setting with the final goal of uncovering relevant mechanosensitive molecular targets that influence stroke outcomes. To that end, experiments are designed to query the effects of RAMT on skeletal myokines (12, 13) in the acute stroke setting.

ABBREVIATIONS: ASIC, acid sensing ion channel; BDNF, brain-derived neurotrophic factor; LSF, laser speckle flowmetry; MCAO, middle cerebral artery occlusion; RAMT, robot-assisted mechanical therapy

[1] These authors contributed equally to this work.

[2] Correspondence: 505 Davis Heart and Lung Research Institute, 473 West 12th Ave., The Ohio State University Wexner Medical Center, Columbus, OH 43210, USA. E-mail: cameron.rink@osumc.edu

doi: 10.1096/fj.201600437R

This article includes supplemental data. Please visit *http://www.fasebj.org* to obtain this information.

MATERIALS AND METHODS

Middle cerebral artery occlusion

All experiments were approved by the Institutional Animal Care and Use Committee of The Ohio State University. Prior to surgery, rats were randomized to either control ($RAMT^-$) or robot-assisted mechanical therapy ($RAMT^+$) treatment groups. Transient (90 min) focal cerebral ischemia was induced in the right hemisphere of 10-wk-old male Wistar rats (Harlan Laboratories, Indianapolis, IN, USA) by the intraluminal suture method of middle cerebral artery occlusion (MCAO) (14). Laser Doppler flowmetry (DRT4; Moor Instruments, Wilmington, DE, USA) was used to confirm successful MCAO (>70% drop in MCA territory cerebral blood flow). A total of 38 rats were used for the study, of which 4 were excluded for insufficient occlusion of the MCA territory, as determined by laser Doppler flowmetry.

MRI

T2-weighted imaging was performed on stroke-affected rats, with a 9.4-T magnetic resonance imaging system (Bruker Daltonics, Billerica, MA, USA) (15, 16). For stroke-volume calculations, raw magnetic resonance images were converted to digital imaging and communications in medicine (DICOM) format and imported into Osirix software (Osirix, Bernex, Switzerland). After matched contrast enhancement of images, digital planimetry was performed by a blinded observer to delineate the infarct area in 1-mm coronal brain slices encompassing the entire neocortex. Infarct areas from brain slices were summed, multiplied by slice thickness, and corrected for edema-induced swelling to determine infarct volume (17).

RAMT

The timing and duration of RAMT delivery were selected on the basis of published ranges of physiotherapy for stroke patients (18–20), where early intervention is reported to provide maximum benefit in both clinical (21) and preclinical (22) settings. To begin, we sought to assess 30 min of daily RAMT at a 0.5-N load over 10 mm of travel on the stroke-affected (left) gastrocnemius muscle. After MCAO, $RAMT^+$ rats received 30 min of robot-assisted mechanical therapy over the stroke-affected muscle daily for up to 14 d. During RAMT therapy, rats were maintained under isoflurane anesthesia (1.3%) with respiratory rates of 50–60 breaths/min. To control for potential confounding effects of anesthesia, $RAMT^-$ rats received a matching dose of daily isoflurane anesthesia for 30 min. $RAMT^+$ rats received a 0.5-N load from the contact head (8-mm-diameter sphere) (Supplemental Fig. 1) in a linear motion with 10 mm of travel over the stroke-affected gastrocnemius muscle at a frequency of 1 Hz. During $RAMT^-$ or $RAMT^+$ therapy, animal body temperature was maintained at 37 ± 1°C with a heat lamp.

Laser speckle flowmetry

To determine mechanical therapy–induced changes in local blood flow, laser speckle flowmetry (LSF) perfusion mapping was performed over stroke-affected and contralateral hindlimbs on post-MCAO d 7 and 14. During LSF acquisition, rats were maintained under isoflurane anesthesia (1.3%) with respiratory rates of 50–60 breaths/min. Core body temperature was maintained at 37 ± 1°C during LSF testing with a heated operating table. LSF recordings of the stroke-affected and contralateral hindlimb were acquired from a 4-cm^2 field of view with a 785-nm, 100-mW laser with a sampling rate of 50 Hz at a working distance of 18 cm (PeriCam PSI NR System; PeriMed, Stockholm, Sweden). Relative perfusion was calculated from a 1- × 0.25-cm region of interest covering the saphenous artery before its distal bifurcation point.

Locomotor analyses

Treadmill walking speeds for rat gait models are reported in the range of 20–40 cm/s (23). After stroke, however, rats were unable to generate reproducible foot models at these speeds. To accommodate poststroke gait injury, rats were walked at a slower speed of 14 cm/s. They were subjected to 15-min treadmill training sessions for 7 d before MCAO. Baseline data were acquired in the session 24 h before MCAO stroke surgery. Poststroke gait data were acquired on d 7 after MCAO. The TreadScan system (CleverSys, Inc., Reston, VA, USA) consists of a motor-driven transparent treadmill belt with a high-speed digital video camera recording the ventral view of the rat at 100 frames/s. Foot models were traced within TreadScan software (24). Automated software calculations from baseline and poststroke d 7 foot models were used to quantify track width (mm), percentage of time quad support, and stride length.

Open-field test

Spontaneous locomotor activity was assessed at baseline and on poststroke d 14 with an open-field test (15). Rats were placed in the center of a 1 m^2 open field and allowed to move freely for 5 min while being recorded overhead with AnyMaze video tracking software (version 4.5; Stoelting Co., Wood Dale, IL, USA). Software was used to divide the open field into 4 equal zones (0.5 m^2). The time spent in each zone was recorded. In addition, total distance traveled (m), total time mobile (s), and time freezing (s) were calculated by software. After open-field testing on d 14, rats were euthanized, and stroke-affected and contralateral gastrocnemius muscle were procured for downstream gene and protein expression analyses.

RNA isolation and real-time quantitative PCR

Total RNA was extracted from stroke-affected and contralateral gastrocnemius muscle of $RAMT^-$ and $RAMT^+$ rats ($n = 7$) (25). In brief, isolated total RNA was reverse transcribed by using oligo-dT primer and Superscript III (Thermo Fisher Scientific, Waltham, MA, USA) to generate cDNA. Myostatin and BDNF gene expression was quantified by real-time PCR assay using SYBR Green-I (Thermo Fisher Scientific). Gene expression was normalized to 18s ribosomal RNA expression and is reported as fold change in stroke-affected gastrocnemius as compared to pair-matched contralateral. The following primer sets were used: rMSTN (forward) 5′–GGAATCGCGGTGCTGTCGCT–3′, (reverse) 5′–GCCGAGCCTCTGGGGTTTGC–3′, rBDNF (forward) 5′–GGGTGAAACAAAGTGGCTGT–-3′, rBDNF (reverse) 5′–ATGTTGTCAAACGGCACAAA–3′.

Immunohistochemistry

Immunohistochemical determination of protein expression in stroke-affected and contralateral gastrocnemius muscle was performed (14). Contralateral (right) and stroke-affected (left) gastrocnemius muscle of poststroke d 14 ($n = 7$) was embedded in Optimal Cutting Temperature Compound (Sakura, Torrance, CA, USA) and frozen. Blocks were cut in longitudinal sections (10 μm) and mounted onto charged slides. Sections were blocked in

10% normal serum, followed by incubation with primary antibodies against either myostatin (1:100; R&D Systems, Minneapolis, MN, USA) or BDNF (1:100; EMD Millipore, Darmstadt, Germany). Signal was visualized by reaction with fluorescent secondary antibodies (Thermo Fisher Scientific). Images were captured with an Axiovert 200M microscope (Zeiss, Jena, Germany), and expression was quantified as the percentage of area from the average of 3 fields of view per section using the AutoMeasure plugin within Axiovert software (ver. 4.8; Zeiss) (14).

Skeletal muscle cytokine array

Additional rats were subjected to MCAO and randomized to RAMT$^-$ or RAMT$^+$ treatment groups (n = 4) for 7 d, as previously described. After 7 d, the rats were euthanized, and proteins from stroke-affected gastrocnemius were isolated and pooled to query cytokine expression in response to RAMT. Cytokine levels in stroke-affected muscle tissue were measured with the Proteome Profiler Rat Cytokine Array Panel A Array Kit (R&D Systems) according to the manufacturer's instructions. Optical density of each signal was measured with ImageJ software and calculated based on the positive controls. Top candidate proteins that were up- and down-regulated in stroke-affected RAMT$^+$ as compared to RAMT$^-$ gastrocnemius were validated in poststroke d 7 tissues by immunohistochemistry, as previously described, with antibodies against IL-1ra (Abcam, Cambridge, MA, USA) or IP-10/CXCL10 (LifeSpan Biosciences, Seattle, WA, USA).

Statistical analyses

Data are reported as means ± SD. Comparisons between means were tested by 1-way ANOVA with Tukey's *post hoc* test or Student's t test, as appropriate. A value of $P < 0.05$ was considered statistically significant.

RESULTS

Design of the RAMT device was aimed at controlling the force, frequency, and form of mechanical therapy applied to stroke-affected muscle (**Fig. 1**). A software-controlled,

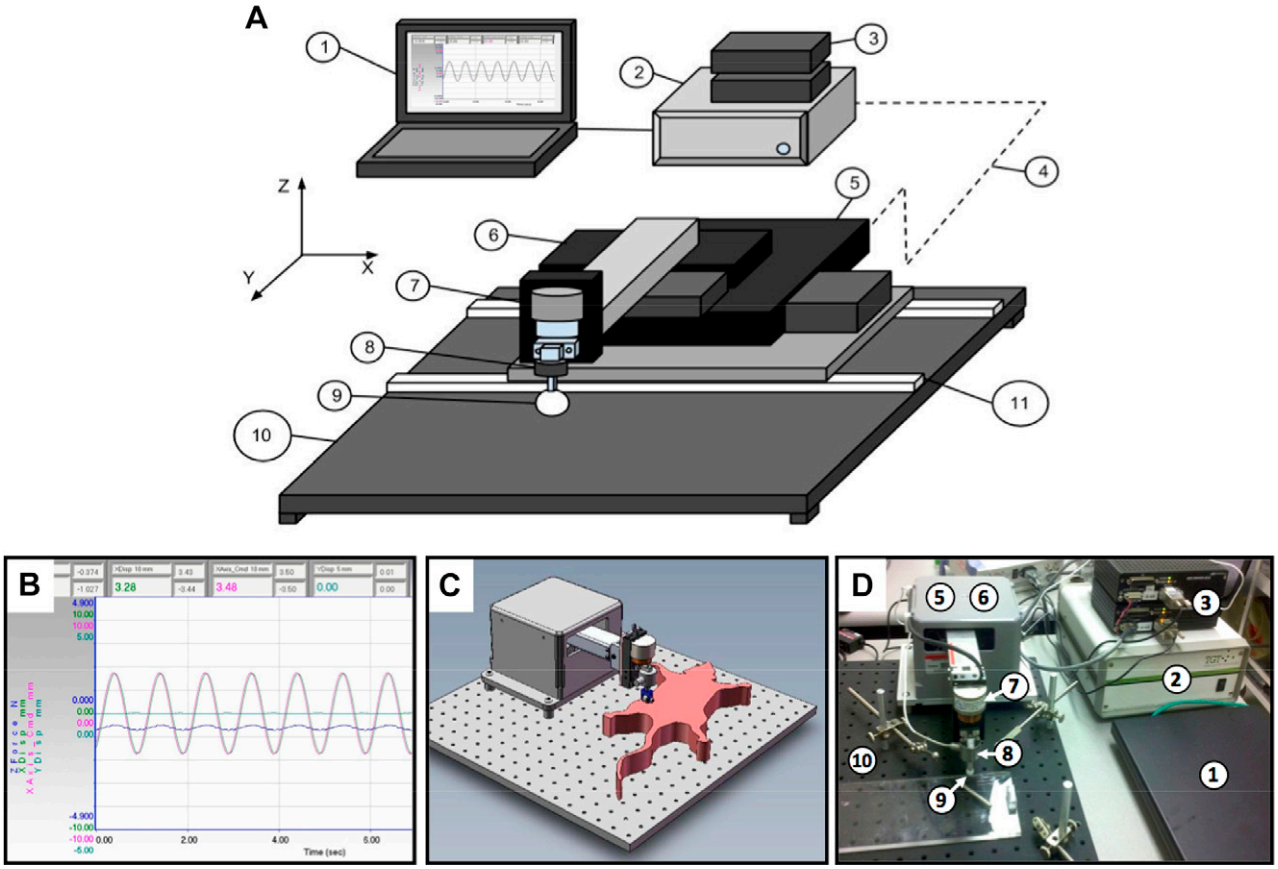

Figure 1. Robot-assisted mechanical therapy (RAMT) hardware. *A*) The RAMT apparatus is controlled by a customized version of software fabricated to our design (*1*) and connected to a controller (*2*). A pair of servo amplifiers (*3*) drive the *x*- and *y*-axis motorized linear stages (*5*, *6*). A servo amplifier integrated to the controller drives the *z*-axis voicecoil stage (*7*). The controller monitors (*4*) stage and contact head (*9*) positions using optical sensors (not shown) mounted on each of the stages. A load cell (*8*) mounted on the *z*-axis stage (*7*) provides the force feedback signal used to monitor and control the load applied by the stage. The bottom stage is mounted on rails (*11*) that allow the stack to be positioned on either side of a breadboard-type base plate (*10*). *B*) The customized software platform enables programmable control of RAMT load (force), pattern (linear, orbital, vibratory), and duration. The RAMT paradigm employed for the current study was 30 min linear motion (10 mm) at a frequency of 1 Hz and a constant load of 0.5 N over the stroke-affected hindlimb. *C*, *D*) The RAMT hardware was conceptualized and prototyped using computer-aided design (*C*) before delivery of final hardware (*D*).

programmable load cell maintains a constant force over a nonuniform target muscle (*i.e.*, gastrocnemius). Rats were subjected to 90 min of MCAO, as confirmed by a >70% reduction in MCA territory perfusion, according to laser Doppler flowmetry (Supplemental Fig. 2). No significant difference was observed in stroke lesion volume between rats randomized to the RAMT$^-$ or RAMT$^+$ groups.

RAMT improved paretic limb perfusion

In the literature, the effect of massage on blood flow at the site of physiotherapy is mixed (26–28). We sought to test the hypothesis that RAMT improves perfusion at the site of application using noninvasive LSF. At poststroke d 7, a modest but nonsignificant trend for higher perfusion was observed in the stroke-affected hindlimb of rats treated with RAMT (**Fig. 2**). After 14 consecutive days of poststroke therapy, RAMT$^+$ significantly increased perfusion in the stroke-affected limb [5.23 ± 0.78 perfusion units (PU)] compared to that of the contralateral control (3.46 ± 0.57 PU; Fig. 2*B*). On poststroke d 14, RAMT$^+$ rats also had significantly greater blood flow in the stroke-affected hindlimb, compared to the site-matched stroke-affected hindlimb of RAMT$^-$ controls (3.54 ± 0.41 PU).

RAMT attenuated stroke-induced locomotor and sensorimotor deficits

Experiments were designed to test the hypothesis that daily application of reproducible manual therapy by RAMT improves poststroke functional recovery. Gait and sensorimotor testing systems employed automated software analyses to remove observer bias. Poststroke d 7 locomotor deficit compared to baseline in RAMT$^-$ rats resulted in increased quad support time (3.9 ± 1.0 to 9.0 ± 1.5%), and decreased stride length (131.4 ± 17.2 to 84.2 ± 6.4 mm) (**Fig. 3*A***). Daily RAMT$^+$ after stroke improved track width (RAMT$^-$, 36.1 ± 3.6 mm *vs.* RAMT$^+$, 40.4 ± 2.6 mm), quad support time (RAMT$^-$, 9.0 ± 1.5% *vs.* RAMT$^+$, 4.1 ± 0.9%), and stride length (RAMT$^-$, 84.2 ± 6.4 mm *vs.* RAMT$^+$, 102.3 ± 6.7 mm) (Fig. 3*B*). An open-field test was used to evaluate spontaneous locomotion and exploratory activity in rats (29, 30). A quadrant grid, representing 4 equal-sized zones in the open field, was implemented within the Any-Maze software (Stoelting Co.) to evaluate RAMT-dependent changes in exploration activity (**Fig. 4*A***). Heat map occupancy plots from RAMT$^-$ and RAMT$^+$ groups were averaged from all animals in each group. RAMT$^+$ exploratory activity resulted in a more equal distribution of time spent in each of the 4 zones on poststroke d 14 (Fig. 4*B*), with significantly more time spent in zone 4, as compared with their RAMT$^-$ counterparts (74.3 ± 18.3 *vs.* 45.6 ± 28.1 s). Furthermore, RAMT$^+$ rats moved greater distances (24.4 ± 5.0 *vs.* 15.2 ± 7.7 m), spent more time mobile (209.7 ± 24.0 *vs.* 148.0 ± 58.0 s), and less time frozen (49.7 ± 19.8 *vs.* 92.4 ± 30.0 s) *vs.* RAMT$^-$ controls after stroke (Fig. 4*C*).

RAMT attenuated the stroke-induced increase in gastrocnemius myostatin expression

Myostatin, chronically up-regulated in skeletal muscle after ischemic stroke, is an inhibitor of myogenesis (31). We sought to test whether RAMT acutely blunts stroke-induced myostatin expression in the gastrocnemius. On poststroke d 14, myostatin mRNA expression was 39.1% lower in RAMT$^+$ stroke-affected paretic gastrocnemius muscle as compared to RAMT$^-$ controls (**Fig. 5*A***).

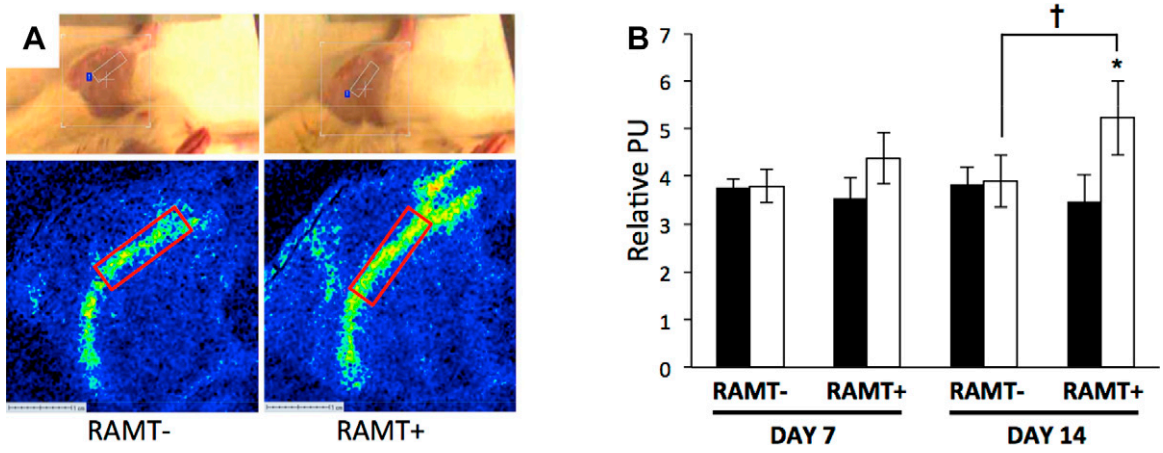

Figure 2. RAMT improves perfusion in stroke-affected gastrocnemius muscle. *A*) Perfusion maps covering the stroke-affected and contralateral saphenous artery were acquired immediately after 30 min of RAMT on poststroke d 7 and 14 (poststroke d 14 shown). Top: rat in supine position with a software-defined bounding box covering the stroke-affected gastrocnemius. Perfusion (relative perfusion units, PU) was quantified from a software-defined region of interest (10 × 1.25 mm) placed over the RAMT site that is inclusive of the femoral artery that supplies the gastrocnemius muscle. *B*) Mean PU in stroke-affected hindlimb of RAMT$^+$ rats was significantly higher than that of the pair-matched contralateral hindlimb on poststroke d 14. Furthermore, mean PU was significantly higher in stroke-affected hindlimb of RAMT$^+$ rats as compared with stroke-affected hindlimb of RAMT$^-$ rats on poststroke d 14. Data are means ± SD (n = 4). Black bars, contralateral limbs; white bars, stroke-affected limbs. *$P < 0.05$, RAMT$^+$ stroke affected *vs.* contralateral; $^\dagger P < 0.05$, RAMT$^+$ stroke affected *vs.* RAMT$^-$ stroke affected.

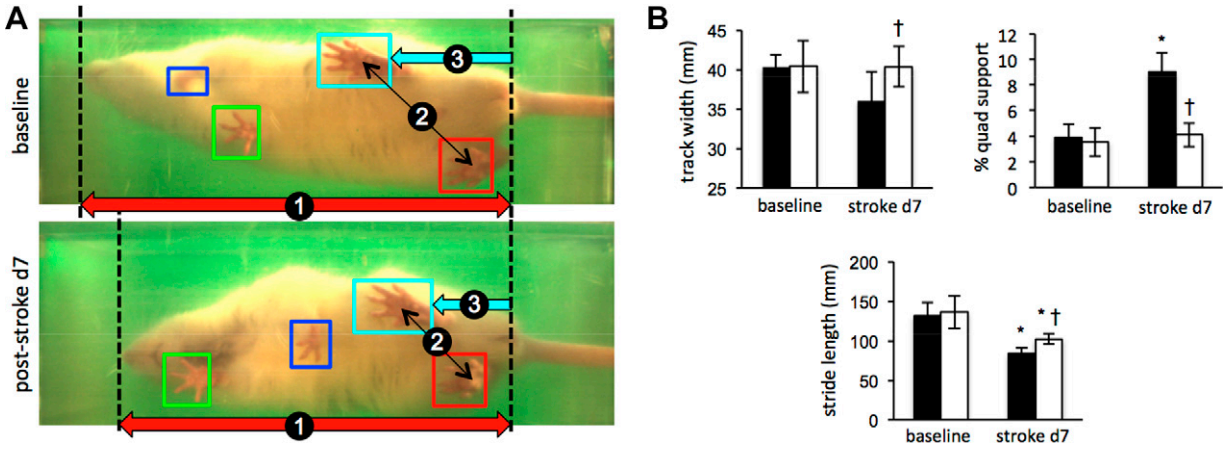

Figure 3. RAMT improves poststroke gait function. *A*) Representative still frames matched for stride position in control (RAMT$^-$) rat at baseline and on poststroke d 7 demonstrate hunched posture (*1*), reduced rear track width (*2*), and shorter stride length (*3*). *B*) Compared to RAMT$^-$ controls (black bars), RAMT$^+$ rats (white bars) had significantly increased track width, spent less time in quad support, and had a longer stride at poststroke d 7. Data are means ± SD ($n = 7$). *$P < 0.05$ *vs.* baseline within group; †$P < 0.05$ *vs.* RAMT$^-$ at the same timepoint.

Histological visualization of myostatin on poststroke d 14 also revealed increased myostatin protein expression in stroke-affected gastrocnemius of RAMT$^-$ rats, when matched to their contralateral gastrocnemius (Fig. 5*B*, *C*). RAMT$^+$ rats were spared such adverse induction of myostatin. Furthermore, myostatin expression was significantly lower in the RAMT-treated gastrocnemius on poststroke d 14 *vs.* that in pair-matched contralateral nontreated gastrocnemius muscle.

RAMT protected against the loss of BDNF in stroke-affected gastrocnemius

BDNF is essential for maintaining physiological mechanotransduction signaling (32). We sought to test the effects of RAMT on BDNF expression in stroke-affected skeletal muscle. RAMT significantly increased BDNF mRNA expression nearly 40-fold in stroke-affected gastrocnemius, as compared to RAMT$^-$ controls (**Fig. 6*A***). Immunohistochemical localization of BDNF in gastrocnemius muscle revealed that RAMT$^+$ protected against stroke-induced loss of BDNF in the paretic limb. BDNF levels were significantly lower in stroke-affected gastrocnemius muscle than in their contralateral counterparts on poststroke d 14 (5.4 ± 3.9 *vs.* 9.37 ± 2.14%). Conversely, no difference in BDNF expression was observed between stroke-affected and contralateral gastrocnemius of RAMT$^+$-treated rats (9.9 ± 3.5 *vs.* 12.5 ± 6.9%). BDNF levels, however, were 2.3 times higher in stroke-affected gastrocnemius of RAMT$^+$ rats, compared with that of RAMT$^-$ rats (Fig. 6*B*, *C*).

Stroke-affected gastrocnemius cytokine profile in response to RAMT

To identify additional RAMT-sensitive targets, we queried an array of skeletal muscle cytokines on poststroke d 7 (**Fig. 7*A*** and **Table 1**). Cytokines on the array with the greatest fold change in response to 7 d of RAMT physiotherapy were validated histologically. RAMT$^+$ significantly induced expression of IL-1 receptor agonist (IL-1ra) and repressed the stroke-precipitated rise in IFN-γ-induced protein 10 (IP-10/CXCL10), as compared to RAMT$^-$ controls (**Fig. 7*B***, ***C***).

DISCUSSION

In light of the expectation that stroke prevalence in the United States will increase by 20.5% between 2012 and 2030 (1), the significance of poststroke physiotherapy and rehabilitative services will substantially grow over time. However, evidence-based research and our understanding of the underlying mechanisms for effective poststroke rehabilitation remain scant. Nearly 1000 randomized clinical trials in stroke rehabilitation over the past 30 yr have tested a range of neurorehabilitation techniques that include repetitive task training, biofeedback, constraint-induced movement, robotics, and virtual reality (33). Despite these efforts, systematic reviews of widely used neurophysiological approaches in stroke have reported mixed outcomes and evidence suggesting no superiority for one approach over another (5). Furthermore, basic science and preclinical research efforts have not been successfully leveraged to identify mechanisms of action in support of physiotherapy and poststroke rehabilitative care (34). In modern health care systems that emphasize accountable care and evidence-based outcomes, the problem remains that therapists in neurology base their assumptions about intervention on philosophical perspectives, which determine how patients are assessed and treated (5).

In the United States, massage therapy is increasingly used as an adjunct to conventional care for musculoskeletal injury recovery (7, 9). In the context of stroke rehabilitative therapy, awareness of massage therapy is limited to systematic review as a component of complex

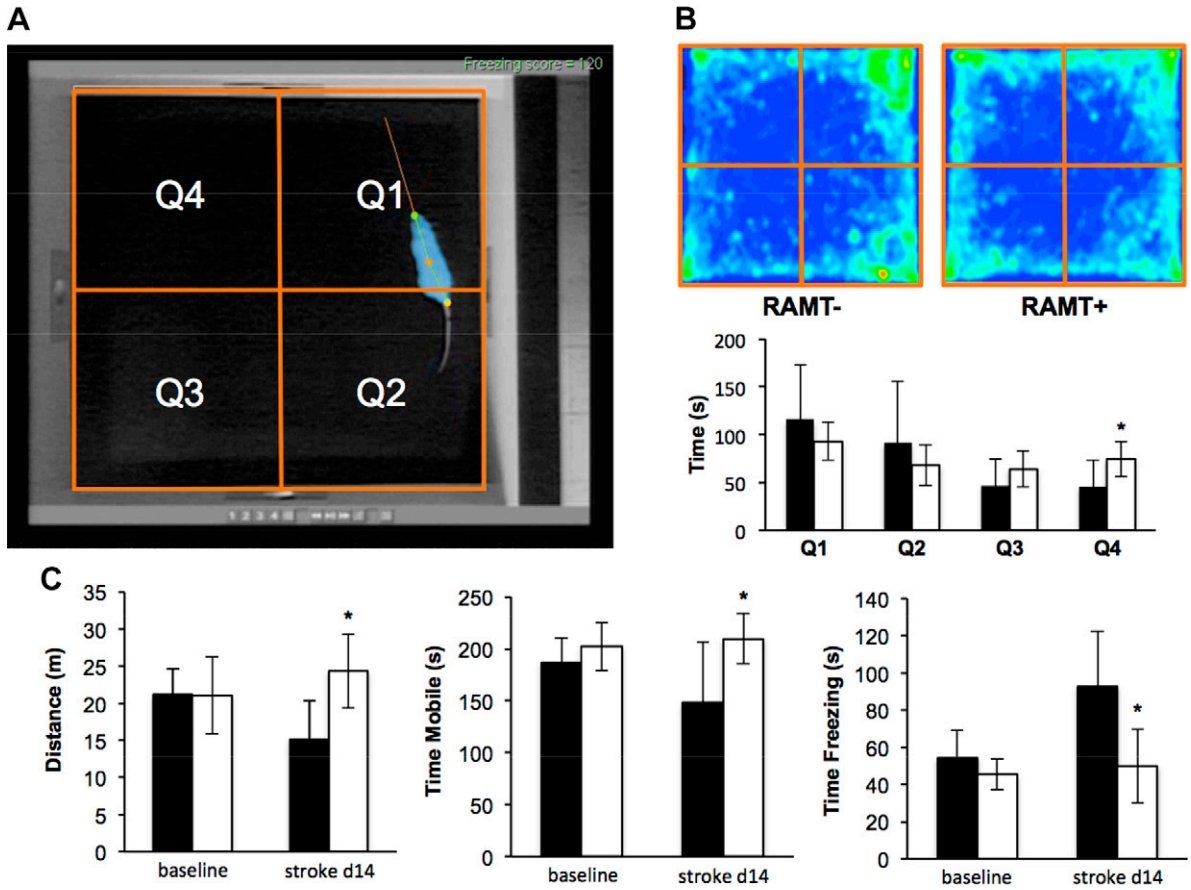

Figure 4. RAMT improves poststroke sensorimotor function. *A*) Representative screen capture of baseline RAMT$^-$ (control) rat with software overlay tracking head (green dot), middle body (orange dot), tail (yellow dot), and motion vector (orange line) in real time. Software was used to divide the open field into 4 quadrants (orange boxes Q1–Q4) for tracking the amount of time spent in each zone during the test. *B*) Average heat map of RAMT$^-$ and RAMT$^+$ rats during field test on poststroke d 14. A video tracking system calculated mean time spent in each zone (RAMT$^-$, black bars; RAMT$^+$, white bars). *C*) Compared to RAMT$^-$ rats, RAMT$^+$ rats traveled greater distance and spent more time mobile and less time freezing on poststroke d 14. Data are means ± SD ($n = 7$). *$P < 0.05$ *vs.* RAMT$^-$ at same timepoint.

traditional Chinese medicine (8). Like other neurorehabilitation techniques, mechanical therapy research to date lacks rigorous preclinical testing for the development of hypothesis-driven, evidence-based research studies. To directly address this problem, we developed a software-controlled RAMT device that can reproducibly deliver the force, frequency, duration, and implementation style of mechanical therapy. This work represents a maiden effort

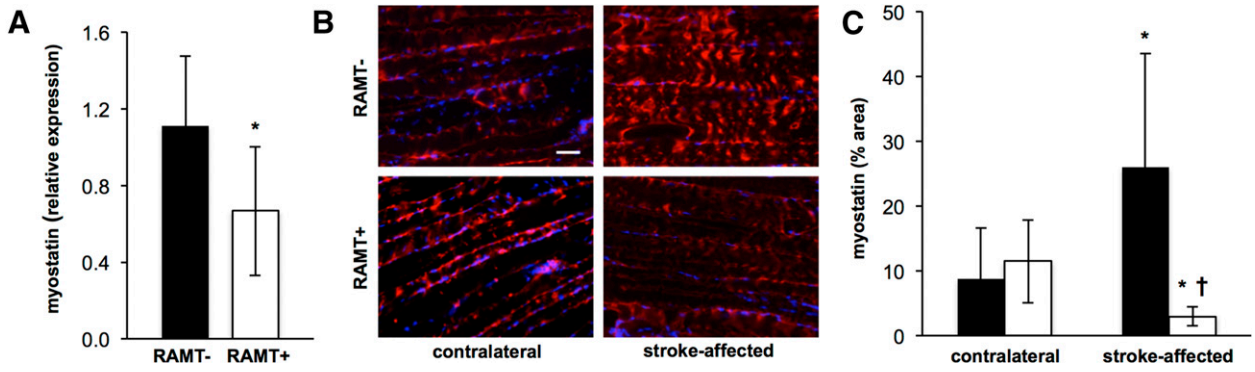

Figure 5. Poststroke myostatin expression is down-regulated in stroke-affected gastrocnemius muscle after RAMT treatment. *A*) Myostatin mRNA expression in stroke-affected gastrocnemius muscle was significantly lower in RAMT$^+$ *vs.* RAMT$^-$ rats on poststroke d 14. *$P < 0.05$ *vs.* RAMT$^-$. *B*) Representative myostatin (red) in contralateral and stroke-affected gastrocnemius muscle on poststroke d 14. Sections counterstained with DAPI (blue). Scale bar, 50 μm. *C*) Quantification (% area) of myostatin expression in contralateral and stroke-affected gastrocnemius muscle of RAMT$^-$ (black bars) and RAMT$^+$ (white bars) rats. Data are means ± SD ($n = 7$). *$P < 0.05$ *vs.* contralateral within group; $^{\dagger}P < 0.05$ *vs.* stroke-affected RAMT$^-$.

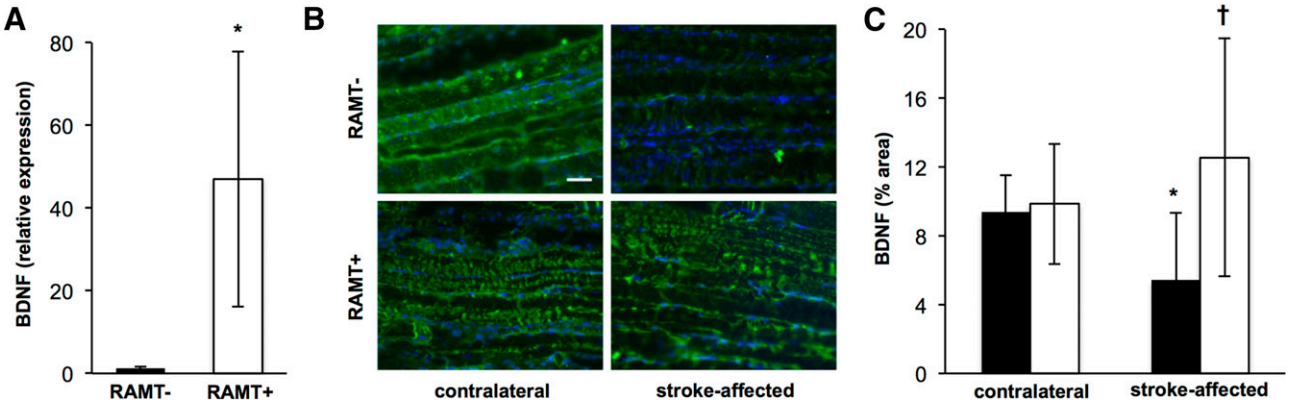

Figure 6. RAMT protects against stroke-induced loss of BDNF in skeletal muscle. *A*) BDNF mRNA expression in stroke-affected gastrocnemius muscle was significantly higher in $RAMT^+$ *vs.* $RAMT^-$ rats on poststroke d 14. $^*P < 0.05$ *vs.* $RAMT^-$. *B*) BDNF (green) immunostaining in contralateral and stroke-affected gastrocnemius muscle on poststroke d 14. Sections counterstained with DAPI (blue). Scale bar, 50 μm. *C*) Quantification (% area) of BDNF expression in contralateral and stroke-affected gastrocnemius muscle of $RAMT^-$ (black bars) and $RAMT^+$ (white bars) rats. Data are means ± SD ($n = 7$). $^*P < 0.05$ *vs.* contralateral within group; $^\dagger P < 0.05$ *vs.* stroke-affected $RAMT^-$.

to employ this device as a tool to quantitatively assess the efficacy of mechanical therapy on poststroke functional outcome and identify mechanical therapy-sensitive molecular targets. It is known that MCAO acutely worsens electromyography-measured burst duration (35) and causes a loss of muscle mass (36) in stroke-affected gastrocnemius muscle within 7 d after cerebral ischemia in rats. The justification for acute rehabilitation is evidenced, both in our outcomes as well as in the primary literature, where physiotherapy within 30 d of stroke is believed to be critical to capitalize on early remodeling events of neurogenesis, plasticity, and synaptogenesis in stroke-affected brain (33).

Whereas the RAMT device is capable of different types of manual therapy, including orbital and vibratory motions, the current work was focused on a single force, frequency, and modality (linear motion) of RAMT delivery to improve poststroke functional recovery within a 2-wk testing period. Future efforts will test dose-response effects of differing RAMT treatment paradigms to determine their effects on poststroke functional outcomes. A limitation of the RAMT approach is the requirement to maintain animals under anesthesia during the manual therapy session. As it relates to anesthesia effects, repeated exposure to isoflurane is known to cause long-lasting, but nonpermanent, impairment of long-term potentiation in Wistar rats (37). Furthermore, object recognition and reversal learning are known to be significantly impaired in young rats receiving repeated isoflurane exposure, but not adult rats (> P60) as used in the current work (38). To mitigate risk of anesthesia confounding outcomes in our study we elected to match exposure time and duration of anesthesia in our control ($RAMT^-$) group. In addition, sensorimotor testing on d 7 and 14 was performed 24 h after the last anesthesia episode, and just before the subsequent day's exposure (d 7) or euthanasia (d 14) to allow for maximum recovery time.

To characterize the peripheral musculoskeletal response to mechanical therapy after stroke injury, we queried expression of stroke and mechanosensitive myokines. Myostatin is a transforming growth factor β (TGF-β) family member known to be a negative regulator of muscle size by arresting muscle progenitor cell expansion (39). In the human condition, stroke-induced sarcopenia is associated with elevated myostatin expression in stroke-affected muscle. Specifically, myostatin expression was reported to be chronically induced, with 40% higher expression in paretic as compared to nonparetic vastus lateralis of stroke survivors (31). Poststroke resistive training in the same cohort was found to lower myostatin expression in stroke-affected muscle. In the current work, we identified a rapid induction of myostatin in stroke-affected skeletal muscle after ischemic stroke that suggests a deliberate and controlled biological process for stroke-induced sarcopenia that occurs within an acute time period (14 d). Daily RAMT physiotherapy was effective in attenuating this rise. As is the case with resistive training that attenuated chronic myostatin expression in humans (31), massage therapy is known to activate mechanotransduction signaling pathways (9). How RAMT affects these pathways and the significance of mechanotransduction signaling on myostatin expression remain to be elucidated.

RAMT of the stroke-affected gastrocnemius muscle also prevented stroke-induced loss of BDNF, a neurotrophic factor that, despite its name, is widely expressed across tissues and cell types (40). Although additional studies are needed to identify the RAMT-dependent mechanisms that protect against stroke-induced loss of BDNF, evidence suggests that BDNF plays a critical role in both physiological and reparative processes in skeletal muscle. Indeed, BDNF is known to directly affect neurosensory mechanotransduction signaling *via* regulation of acid-sensitive ion channel (ASIC)-2. Specifically, McIlwrath *et al.* (41) reported a loss of ASIC2 channel expression in sensory neurons of BDNF deficient mice. In the context of injury, gastrocnemius-derived BDNF is known to reduce motor functional deficits in rats with a transected spinal cord (42). Furthermore, in mice with conditional depletion of BDNF from skeletal muscle cells, satellite cell repair of

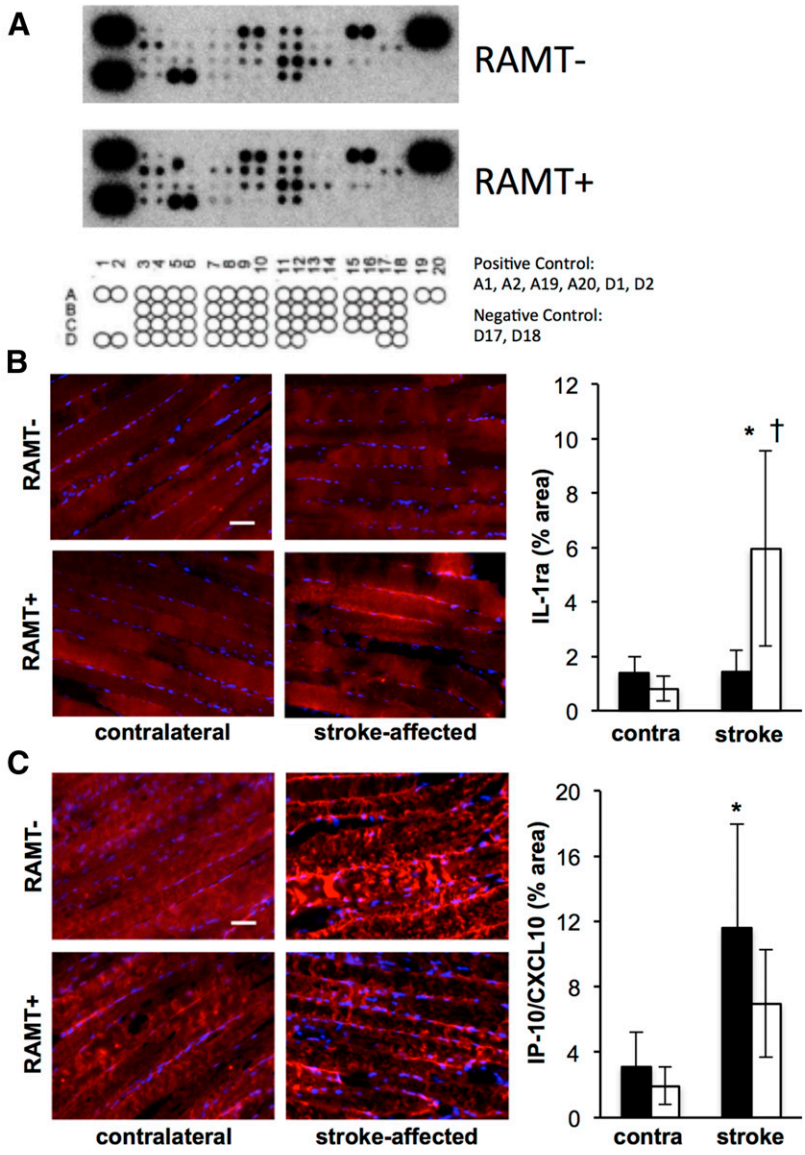

Figure 7. Cytokine profile of stroke-affected skeletal muscle in response to RAMT. *A*) Images of chemiluminescent intensity from the cytokine array. Rat cytokine array coordinates indicate the position of cytokines measured in **Table 1**. Optical density of each signal was measured by ImageJ, and values were calculated based on the signal intensity of the positive controls from the same membrane. *B*, *C*) Immunohistology was used to validate targets with the greatest fold-change up (IL-1ra, *B*) and down (IP-10/CXCL10, *C*). Immunohistology was quantified as % area in contralateral and stroke-affected gastrocnemius muscle of RAMT^{-} (black bars) and RAMT^{+} (white bars) rats. Data are means ± SD ($n = 4$). *$P < 0.05$ *vs.* contralateral within group, $^{\dagger}P < 0.05$ *vs.* stroke-affected RAMT^{-}.

cardiotoxin-induced injury is compromised with lowered expression of regenerative factors including pair box 7 (Pax7), myogenic differentiation (MyoD), myogenin, and embryonic myosin heavy chain (emb-MyHC) (43). Taken together, outcomes point toward mechanosensitive BDNF as a key player in peripheral skeletal muscle regeneration postinjury. Massage therapy has been reported to increase plasma BDNF levels in humans (44). To our knowledge, the current work is the first to describe stroke-induced loss of BDNF in affected skeletal muscle. That the stroke-induced loss of BDNF expression occurred within 14 d of stroke injury further suggests that pathophysiological pathways affecting poststroke functional recovery are enacted acutely and supports the concept of acute rehabilitative physiotherapy.

A growing body of literature supports evidence of pathophysiological inflammatory cytokine signaling in skeletal muscle after a stroke (45, 46). In the current work, query of skeletal muscle cytokine expression on poststroke d 7 uncovered novel targets that are acutely induced by stroke and are differentially expressed in response to RAMT physiotherapy. IP-10/CXCL10 is a chemotactic cytokine that recruits leukocytes and promotes inflammation in response to skeletal muscle myopathy (47). Expression of IP-10/CXCL10 was significantly higher in stroke-affected skeletal muscle on poststroke d 7, but was attenuated by daily RAMT physiotherapy. This observation uncovers a novel testable hypothesis that stroke-induced IP-10/CXCL10 signaling attracts leukocytes to skeletal muscle that contribute to inflammation and stroke-induced sarcopenia. In this paradigm, RAMT can be used as a tool to test the significance of IP-10/CXCL10 chemotactic signaling in poststroke limb sarcopenia. The cytokine array experiment also identified an RAMT-dependent increase in anti-inflammatory cytokine IL-1ra expression. IL-1ra is the receptor antagonist to the potent proinflammatory cytokine IL-1 (48). In the CNS, proinflammatory IL-1 delivery to brain represses the induction of BDNF associated with contextual learning (49). Injection of IL-1ra prevents this loss; restoring BDNF to

TABLE 1. *Skeletal muscle cytokine profile on poststroke d 7*

Cytokine/chemokine	Position	RAMT$^-$	RAMT$^+$	Fold change
CINC-1	A3, A4	0.17	0.2	1.21
CINC-2α/β	A5, A6	ND	ND	—
CINC-3	A7, A8	0.03	0.02	0.61
CNTF	A9, A10	0.5	0.67	1.32
Fractalkine	A11, A12	0.23	0.33	1.45
GM-CSF	A13, A14	0.03	0.04	1.41
sICAM-1	A15, A16	0.73	0.84	1.15
IFN-γ	A17, A18	ND	ND	—
IL-1α	B3, B4	0.29	0.43	1.47
IL-1β	B5, B6	0.05	ND	—
IL-1ra	*B7, B8*	*0.05*	*0.12*	*2.25*
IL-2	B9, B10	0.16	0.34	2.16
IL-3	B11, B12	0.22	0.36	1.61
IL-4	B13, B14	0.05	ND	—
IL-6	B15, B16	ND	ND	—
IL-10	B17, B18	0.14	0.17	1.24
IL-13	C3, C4	0.14	0.22	1.65
IL-17	C5, C6	0.12	0.19	1.61
IP-10/CXCL10	*C7, C8*	*0.04*	*0.03*	*0.73*
LIX	C9, C10	0.12	0.22	1.94
L-Selectin	[^{11}C], C12	0.52	0.65	1.24
MIG	[^{13}C], C14	0.19	0.15	0.8
MIP-1α	C15, C16	0.07	0.08	1.12
MIP-3α	C17, C18	ND	ND	—
RANTES	D3, D4	0.15	0.25	1.69
Thymus chemokine	D5, D6	0.8	0.88	1.1
TIMP-1	D7, D8	0.04	0.07	1.55
TNF-α	D9, D10	ND	ND	—
VEGF	D11, D12	0.3	0.29	0.97

ND, not detected. Italicized cytokines were validated by immunohistochemistry (Fig. 7*B*, *C*).

physiological levels and preventing memory impairment (50). The link between IL-1ra and BDNF in skeletal muscle is unfounded and opens an interesting new direction. Whether RAMT-dependent induction of IL-1ra is upstream and required for BDNF up-regulation in stroke-affected skeletal muscle is a novel testable hypothesis.

In summary, the current work represents a maiden effort to develop and test an RAMT system that enables the objective study of mechanical physiotherapy after acute ischemic stroke. Outcomes identify an early and effective window of opportunity for mechanical therapy to improve poststroke gait and sensorimotor function. Furthermore, the query for a mechanistic basis of this benefit uncovered novel molecular targets that affect sarcopenia (myostatin), skeletal muscle regeneration (BDNF), and inflammatory signaling events (IL-1ra, CXCL10) in the stroke-affected limb. Taken together, the results suggest that the acute impact of stroke injury extends beyond the CNS to include stroke-affected skeletal muscle and that mechanical therapy is effective in abrogating such injury. FJ

ACKNOWLEDGMENTS

The authors thank Phil Levesque (Instron Term, Norwood, MA, USA) for support with design and fabrication of the RAMT system. Supported in part by U.S. National Institutes of Health, National Institute of Neurological Disorders and Stroke Grants NS42617 (to C.K.S.) and NS085272 (to C.R., S.K., and A.H.A.), and American Heart Association Scientific Development Grant 12SDG11780023 (to C.R.). The authors declare no conflicts of interest.

AUTHOR CONTRIBUTIONS

C. K. Sen and C. Rink conceptualized the RAMT device; C. K. Sen, S. Khanna, and C. Rink designed the research; S. Khanna, H. Harris, R. Stewart, M. Balch, M. Heigel, S. Teplitsky, S. Gnyawali, and C. Rink performed the experiments; C. K. Sen, S. Khanna, M. Heigel, S. Gnyawali, and C. Rink analyzed and interpreted the data; C. K. Sen, S. Khanna, R. Stewart, S. Gnyawali, and C. Rink prepared the figures; and C. K. Sen, S. Khanna, and C. Rink prepared the manuscript.

REFERENCES

1. American Heart Association Statistics Committee and Stroke Statistics Subcommittee. (2013) Heart disease and stroke statistics: 2013 update: a report from the American Heart Association. *Circulation* **127**, e6–e245; Correction: **127**, e841
2. American Heart Association Council on Cardiovascular Nursing and the Stroke Council. (2010) Comprehensive overview of nursing and interdisciplinary rehabilitation care of the stroke patient: a scientific statement from the American Heart Association. *Stroke* **41**, 2402–2448
3. Langhorne, P., Bernhardt, J., and Kwakkel, G. (2011) Stroke rehabilitation. *Lancet* **377**, 1693–1702
4. Lennon, S., Baxter, D., and Ashburn, A. (2001) Physiotherapy based on the Bobath concept in stroke rehabilitation: a survey within the UK. *Disabil. Rehabil.* **23**, 254–262
5. Kollen, B. J., Lennon, S., Lyons, B., Wheatley-Smith, L., Scheper, M., Buurke, J. H., Halfens, J., Geurts, A. C., and Kwakkel, G. (2009) The effectiveness of the Bobath concept in stroke rehabilitation: what is the evidence? *Stroke* **40**, e89–e97
6. Pomeroy, V. M., and Tallis, R. C. (2000) Need to focus research in stroke rehabilitation. *Lancet* **355**, 836–837
7. Barnes, P. M., Bloom, B., and Nahin, R. L. (2008) Complementary and alternative medicine use among adults and children: United States, 2007. *Natl. Health Stat. Rep.* **10**, 1–23
8. Junhua, Z., Menniti-Ippolito, F., Xiumei, G., Firenzuoli, F., Boli, Z., Massari, M., Hongcai, S., Yuhong, H., Ferrelli, R., Limin, H., Fauci, A., Guerra, R., and Raschetti, R. (2009) Complex traditional Chinese medicine for poststroke motor dysfunction: a systematic review. *Stroke* **40**, 2797–2804
9. Crane, J. D., Ogborn, D. I., Cupido, C., Melov, S., Hubbard, A., Bourgeois, J. M., and Tarnopolsky, M. A. (2012) Massage therapy attenuates inflammatory signaling after exercise-induced muscle damage. *Sci. Transl. Med.* **4**, 119ra13
10. Mori, H., Ohsawa, H., Tanaka, T. H., Taniwaki, E., Leisman, G., and Nishijo, K. (2004) Effect of massage on blood flow and muscle fatigue following isometric lumbar exercise. *Med. Sci. Monit.* **10**, CR173–CR178
11. Hiraiwa, Y., Ariji, Y., Kise, Y., Sakuma, S., Kurita, K., and Ariji, E. (2013) Efficacy of massage treatment technique in masseter muscle hardness: robotic experimental approach. *Cranio* **31**, 291–299
12. Pedersen, B. K., and Febbraio, M. A. (2012) Muscles, exercise and obesity: skeletal muscle as a secretory organ. *Nat. Rev. Endocrinol.* **8**, 457–465
13. Trayhurn, P., Drevon, C. A., and Eckel, J. (2011) Secreted proteins from adipose tissue and skeletal muscle: adipokines, myokines and adipose/muscle cross-talk. *Arch. Physiol. Biochem.* **117**, 47–56
14. Rink, C., Roy, S., Khan, M., Ananth, P., Kuppusamy, P., Sen, C. K., and Khanna, S. (2010) Oxygen-sensitive outcomes and gene expression in acute ischemic stroke. *J. Cereb. Blood Flow Metab.* **30**, 1275–1287
15. Khanna, S., Rink, C., Ghoorkhanian, R., Gnyawali, S., Heigel, M., Wijesinghe, D. S., Chalfant, C. E., Chan, Y. C., Banerjee, J., Huang, Y., Roy, S., and Sen, C. K. (2013) Loss of miR-29b following acute

ischemic stroke contributes to neural cell death and infarct size. *J. Cereb. Blood Flow Metab.* **33**, 1197–1206
16. Khanna, S., Roy, S., Slivka, A., Craft, T. K., Chaki, S., Rink, C., Notestine, M. A., DeVries, A. C., Parinandi, N. L., and Sen, C. K. (2005) Neuroprotective properties of the natural vitamin E alpha-tocotrienol. *Stroke* **36**, 2258–2264
17. Loubinoux, I., Volk, A., Borredon, J., Guirimand, S., Tiffon, B., Seylaz, J., and Meric, P. (1997) Spreading of vasogenic edema and cytotoxic edema assessed by quantitative diffusion and T2 magnetic resonance imaging. *Stroke* **28**, 419–426
18. Ballinger, C., Ashburn, A., Low, J., and Roderick, P. (1999) Unpacking the black box of therapy: a pilot study to describe occupational therapy and physiotherapy interventions for people with stroke. *Clin. Rehabil.* **13**, 301–309
19. Husemann, B., Müller, F., Krewer, C., Heller, S., and Koenig, E. (2007) Effects of locomotion training with assistance of a robot-driven gait orthosis in hemiparetic patients after stroke: a randomized controlled pilot study. *Stroke* **38**, 349–354
20. Kwakkel, G., and Wagenaar, R. C. (2002) Effect of duration of upper- and lower-extremity rehabilitation sessions and walking speed on recovery of interlimb coordination in hemiplegic gait. *Phys. Ther.* **82**, 432–448
21. Salter, K., Jutai, J., Hartley, M., Foley, N., Bhogal, S., Bayona, N., and Teasell, R. (2006) Impact of early vs delayed admission to rehabilitation on functional outcomes in persons with stroke. *J. Rehabil. Med.* **38**, 113–117
22. Liu, Y. H., Zhao, Y., Huang, F. Z., Chen, Y. H., Wang, H. X., Bonney, E., and Liu, B. Q. (2016) Combination of early constraint-induced movement therapy and fasudil enhances motor recovery after ischemic stroke in rats. *Int. J. Neurosci.* **126**, 168–173
23. Canu, M. H., and Falempin, M. (1996) Effect of hindlimb unloading on locomotor strategy during treadmill locomotion in the rat. *Eur. J. Appl. Physiol. Occup. Physiol.* **74**, 297–304
24. Beare, J. E., Morehouse, J. R., DeVries, W. H., Enzmann, G. U., Burke, D. A., Magnuson, D. S., and Whittemore, S. R. (2009) Gait analysis in normal and spinal contused mice using the TreadScan system. *J. Neurotrauma* **26**, 2045–2056
25. Rink, C., Christoforidis, G., Khanna, S., Peterson, L., Patel, Y., Khanna, S., Abduljalil, A., Irfanoglu, O., Machiraju, R., Bergdall, V. K., and Sen, C. K. (2011) Tocotrienol vitamin E protects against preclinical canine ischemic stroke by inducing arteriogenesis. *J. Cereb. Blood Flow Metab.* **31**, 2218–2230
26. Goats, G. C. (1994) Massage: the scientific basis of an ancient art, Part 2: physiological and therapeutic effects. *Br. J. Sports Med.* **28**, 153–156
27. Sefton, J. M., Yarar, C., Berry, J. W., and Pascoe, D. D. (2010) Therapeutic massage of the neck and shoulders produces changes in peripheral blood flow when assessed with dynamic infrared thermography. *J. Altern. Complement. Med.* **16**, 723–732
28. Shoemaker, J. K., Tiidus, P. M., and Mader, R. (1997) Failure of manual massage to alter limb blood flow: measures by Doppler ultrasound. *Med. Sci. Sports Exerc.* **29**, 610–614
29. DeVries, A. C., Nelson, R. J., Traystman, R. J., and Hurn, P. D. (2001) Cognitive and behavioral assessment in experimental stroke research: will it prove useful? *Neurosci. Biobehav. Rev.* **25**, 325–342
30. Herson, P. S., Palmateer, J., Hurn, P. D., and DeVries, A. C. (2011) Evaluating behavioral outcomes from ischemic brain injury. *Neuromethods* **50**, 307–327
31. Ryan, A. S., Ivey, F. M., Prior, S., Li, G., and Hafer-Macko, C. (2011) Skeletal muscle hypertrophy and muscle myostatin reduction after resistive training in stroke survivors. *Stroke* **42**, 416–420
32. Carroll, P., Lewin, G. R., Koltzenburg, M., Toyka, K. V., and Thoenen, H. (1998) A role for BDNF in mechanosensation. *Nat. Neurosci.* **1**, 42–46
33. Stinear, C., Ackerley, S., and Byblow, W. (2013) Rehabilitation is initiated early after stroke, but most motor rehabilitation trials are not: a systematic review. *Stroke* **44**, 2039–2045
34. Krakauer, J. W., Carmichael, S. T., Corbett, D., and Wittenberg, G. F. (2012) Getting neurorehabilitation right: what can be learned from animal models? *Neurorehabil. Neural Repair* **26**, 923–931
35. Li, L., Rong, W., Ke, Z., Hu, X., and Tong, K. Y. (2013) The effects of training intensities on motor recovery and gait symmetry in a rat model of ischemia. *Brain Inj.* **27**, 408–416
36. Choe, M. A., An, G. J., Lee, Y. K., Im, J. H., Choi-Kwon, S., and Heitkemper, M. (2004) Effect of inactivity and undernutrition after acute ischemic stroke in a rat hindlimb muscle model. *Nurs. Res.* **53**, 283–292
37. Long Ii, R. P., Aroniadou-Anderjaska, V., Prager, E. M., Pidoplichko, V. I., Figueiredo, T. H., and Braga, M. F. (2016) Repeated isoflurane exposures impair long-term potentiation and increase basal gabaergic activity in the basolateral amygdala. *Neural Plast.* **2016**, 8524560
38. Zhu, C., Gao, J., Karlsson, N., Li, Q., Zhang, Y., Huang, Z., Li, H., Kuhn, H. G., and Blomgren, K. (2010) Isoflurane anesthesia induced persistent, progressive memory impairment, caused a loss of neural stem cells, and reduced neurogenesis in young, but not adult, rodents. *J. Cereb. Blood Flow Metab.* **30**, 1017–1030
39. Manceau, M., Gros, J., Savage, K., Thomé, V., McPherron, A., Paterson, B., and Marcelle, C. (2008) Myostatin promotes the terminal differentiation of embryonic muscle progenitors. *Genes Dev.* **22**, 668–681
40. Yamamoto, M., Sobue, G., Yamamoto, K., Terao, S., and Mitsuma, T. (1996) Expression of mRNAs for neurotrophic factors (NGF, BDNF, NT-3, and GDNF) and their receptors (p75NGFR, trkA, trkB, and trkC) in the adult human peripheral nervous system and nonneural tissues. *Neurochem. Res.* **21**, 929–938
41. McIlwrath, S. L., Hu, J., Anirudhan, G., Shin, J. B., and Lewin, G. R. (2005) The sensory mechanotransduction ion channel ASIC2 (acid sensitive ion channel 2) is regulated by neurotrophin availability. *Neuroscience* **131**, 499–511
42. Gao, L., Li, L. H., Xing, R. X., Ou, S., Liu, G. D., Wang, Y. P., Zhang, H., Gao, G. D., and Wang, T. H. (2012) Gastrocnemius-derived BDNF promotes motor function recovery in spinal cord transected rats. *Growth Factors* **30**, 167–175
43. Clow, C., and Jasmin, B. J. (2010) Brain-derived neurotrophic factor regulates satellite cell differentiation and skeltal muscle regeneration. *Mol. Biol. Cell* **21**, 2182–2190
44. Wu, J. J., Cui, Y., Yang, Y. S., Kang, M. S., Jung, S. C., Park, H. K., Yeun, H. Y., Jang, W. J., Lee, S., Kwak, Y. S., and Eun, S. Y. (2014) Modulatory effects of aromatherapy massage intervention on electroencephalogram, psychological assessments, salivary cortisol and plasma brain-derived neurotrophic factor. *Complement. Ther. Med.* **22**, 456–462
45. Coelho Junior, H. J., Gambassi, B. B., Diniz, T. A., Fernandes, I. M., Caperuto, E. C., Uchida, M. C., Lira, F. S., and Rodrigues, B. (2016) Inflammatory mechanisms associated with skeletal muscle sequelae after stroke: role of physical exercise. *Mediators Inflamm.* **2016**, 3957958
46. Hafer-Macko, C. E., Ryan, A. S., Ivey, F. M., and Macko, R. F. (2008) Skeletal muscle changes after hemiparetic stroke and potential beneficial effects of exercise intervention strategies. *J. Rehabil. Res. Dev.* **45**, 261–272
47. Crescioli, C., Sottili, M., Bonini, P., Cosmi, L., Chiarugi, P., Romagnani, P., Vannelli, G. B., Colletti, M., Isidori, A. M., Serio, M., Lenzi, A., and Di Luigi, L. (2012) Inflammatory response in human skeletal muscle cells: CXCL10 as a potential therapeutic target. *Eur. J. Cell Biol.* **91**, 139–149
48. Arend, W. P., Malyak, M., Guthridge, C. J., and Gabay, C. (1998) Interleukin-1 receptor antagonist: role in biology. *Annu. Rev. Immunol.* **16**, 27–55
49. Barrientos, R. M., Sprunger, D. B., Campeau, S., Watkins, L. R., Rudy, J. W., and Maier, S. F. (2004) BDNF mRNA expression in rat hippocampus following contextual learning is blocked by intrahippocampal IL-1beta administration. *J. Neuroimmunol.* **155**, 119–126
50. Barrientos, R. M., Sprunger, D. B., Campeau, S., Higgins, E. A., Watkins, L. R., Rudy, J. W., and Maier, S. F. (2003) Brain-derived neurotrophic factor mRNA downregulation produced by social isolation is blocked by intrahippocampal interleukin-1 receptor antagonist. *Neuroscience* **121**, 847–853

Received for publication March 25, 2016.
Accepted for publication November 14, 2016.